ISOTHERMAL TURBULENT FLOW ANALYSIS OF AN AERO GAS TURBINE COMBUSTOR

N. Muthuveerappan*, Venkataraman Shankar** and V. Ganesan+

Abstract

Flow field in a practical aero gas turbine combustor is investigated, under isothermal flow conditions. Simulation has been carried out using commercial CFD software, FLUENT. Complete combustor, starting from compressor exit to turbine inlet, has been modelled using hexahedral dominant grid. All the complicated features of the combustor, including the swirler, have been modelled. Based on the isothermal flow analysis results of the baseline configuration, changes had been made to various air injection holes of the combustor liner, to improve the flow field. Modification on the primary and dilution holes of the liner, by incorporating canted chutes, has been studied. The effect of chuted holes on the jet penetration, mass flow distribution on the annuli and pressure loss is presented. Particular emphasis is given to achieving the proper primary zone recirculation pattern and the jet angle during this study.

Introduction

Due to availability of high speed digital computers at relatively low cost, numerical prediction methods have become popular during the last decade. The new market forces in the aeronautical as well as power generation field demand robust and flexible technologies at low cost, in addition to meet the ever increasing stringent environmental standards and the need for higher fuel economy.

So far gas turbine combustor designs are based on empirical correlations and experimental data. As the experimental methods are inherently time consuming and expensive, many researchers have used Computational Fluid Dynamics (CFD) simulations [1, 2, and 3] to overcome the above difficulty. However, most of the initial studies have been limited to the flow field inside the liner [4, 5] or part of the combustor [6]. The solutions obtained by these simulations are strongly dependent on the accuracy levels associated with the definition of boundary condition. Particularly, the effect of the upstream condition on the property of the jet entering the liner and its effect on altering the primary zone flow pattern are well observed [7]. To reduce the above uncertainty, modeling of the entire flow field from compressor exit to turbine inlet has been carried out by the authors [8, 9, and 10] and also by other researchers [11, 12, and 13].

The use of simulation tools even though not perfect have resulted in good improvement in terms of design capability, cost and turn-around time. Parametric studies may be carried out with various geometries to study the effect of these geometries on the combustor performance, which helps in arriving at an optimized design. These optimized designs reduce extensive rig tests and results in very short design cycle.

In this work, parametric studies on different injection hole geometries have been carried out to arrive at more acceptable flow pattern inside the combustor liner, particularly in the primary zone. To enhance the jet penetration without modifying the number of holes or the diameter of the hole - a suitable sized lip has been added to the injection holes. The effect of this geometric feature has been studied to arrive at an acceptable geometry with desired flow field. Since the flow field inside the liner remains more or less the same with isothermal and reacting conditions, the studies have been carried out in isothermal conditions.

CFD Analysis Methodology

Original Geometry

The cross-section of a practical gas turbine combustor geometry used for analysis is given in Fig.1. For the analysis, the complete combustor, from the compressor

* Group Director ** Additional Director and Technical Director
Gas Turbine Research Establishment (GTRE), CV Raman Nagar, Bangalore-560 093, India, Email : muthuvee@gmail.com
+ Professor, Internal Combustion Engine Lab, Department of Mechanical Engineering, Indian Institute of Technology Madras, Chennai-600 036, India
Manuscript received on 16 Dec 2009; Paper reviewed, revised and accepted as a Full Length Contributed Paper on 19 May 2010

exit to turbine entry, has been considered. The combustor has 18 numbers of airblast atomizers for injection of aviation turbine fuel and each of these atomizers is surrounded by an axial flow swirler. The atomizer has two air passages and a passage for fuel. The flow passages of the swirler and the air flow passages of the atomizer have been modeled; however, the fuel passage is specified as wall.

As the combustor is symmetric, a 20 degree sector of the combustor has been considered for analysis with periodic boundary condition being defined at both 0 degree and 20 degree plane. The atomizer is located in the mid-pane at 10 degrees. The outer liner of the combustor has 36 primary holes, 36 secondary holes and 18 dilution holes. Similarly, the inner liner of the combustor also has the same number of holes except that there are 36 dilution holes. Typical disposition of the primary, secondary and dilution holes on outer/inner liner is pictorially shown in Fig.2.

There are 6 struts at an interval of 60 degrees in the pre-diffuser, which has been modeled by assuming 18 uniform struts of equivalent blockage.

All the air entry ports of the combustor liner have been modeled. The geometry of nozzle guide vane at the combustor exit is simplified as a straight duct and sufficient length is provided to enable the boundary condition definition. The combustor has several cooling rings, with many holes of 2mm diameter, for cooling the liner surface. All these holes have been simplified as slots of equivalent area, while modeling the flow. The flow through all the air entry ports and the cooling rings are computed and no boundary condition has been specified.

Modified Geometry

Initial analysis of the baseline model showed some deficiency in the primary and dilution jet penetrations. Shape and size of the air entry ports play a vital role in dictating the depth of penetration in addition to the upstream and downstream conditions [14]. The novelty of the present study is that in addition to the baseline configuration, four different chute configurations have been considered, for improving the jet penetration within the flame tube. As there is a practical difficulty in enlarging the size of these holes beyond the present size, the shape of the hole has been modified. A skirting has been introduced, such that H/D is 0.75. The depth of the skirting is not constant, but the exit of the skirting is canted towards upstream. The cross-section of combustor with chutes is shown in Fig.3.

The schematic representation of the chuted hole is shown in Fig.4.

These configurations are introduced only on primary holes, dilution holes or on both. In addition, the plane of the dilution holes has been shifted axially upstream to the plane of secondary hole replacing the secondary holes. Table-1 shows the list of the configurations analysed and the details of the configuration. The first configuration is with chutes only in the primary holes, the second configuration is with chutes in both primary and dilution holes, the third configuration is with secondary holes being replaced by the dilution holes having chutes and the fourth configuration is similar to third along with chutes in the primary holes. In model-3 and model-4, there are no secondary holes. The proposal for model-3 and model-4, by moving the dilution holes to the plane of secondary hole, is to increase the mixing length available downstream of the dilution hole. The reacting flow analysis and the experimental results of baseline configuration exhibited higher level of temperature non-uniformity at the combustor exit plane. Closing the secondary hole will increase the liner pressure loss marginally in both model-3 and model-4, but it will be a trade-off to get more mixing length. The disposition of the primary and dilution holes, in model-3 and model-4, after moving the dilution holes, can be schematically represented as shown in Fig.5.

Grid

GAMBIT was used to create a combustor mesh which comprises approximately 2 million cells. This hybrid mesh has majority hexahedral cells (77% Hexahedral, 23% of Tetrahedral, prisms and wedges). Most of the flow

Table-1 : Various Configurations Analysed and Their Definition

Model Designation	Primary Holes	Secondary Holes	Dilution Holes
Model-0	Baseline	Baseline	Baseline
Model-1	Chutes	baseline	Baseline
Model-2	Chutes	Baseline	Chutes
Model-3	Baseline	⇐	Chutes
Model-4	Chutes	⇐	Chutes

volume is meshed using hexahedral mesh. However, tetrahedral mesh is used in a small portion of the combustor, where the geometric complexity is high. Fig.6 shows the grid used for analysis.

Mesh has been generated through the swirler vane passages, as shown in Fig.7, as well as through the air passages of the air-blast atomizer. The computational mesh pass through the primary, secondary and the dilution holes and the flow through these holes are computed. The small holes of cooling ring, of 2mm diameter, have been modeled as slot of equivalent area.

Before arriving at the grid size of 2 million cells, grid independence study has been carried out using grids of three different sizes, for the same combustor geometry, viz. 1.5, 2 and 2.5 million cells. The variation of key combustor performance parameter viz. overall total pressure loss, is compared for all of the above grid sizes. It has been found that the variation of pressure loss between 1st and the 2nd grid size is around 0.5%, where as the variation between 2nd and the 3rd set of grid is less than 0.01% in the overall combustor pressure loss. Hence, 2 million grid size is used for subsequent analyses.

Boundary Condition

At the inlet to the combustor, total pressure and total temperature have been specified. The bleed flow from the inner and outer annulus exit has been specified by fixing the exit mass flow rate at the end of the respective annuli using mass flow boundary conditions. At the exit of the combustor, static pressure and target mass flow rate has been specified. All the cooling air flow to the turbine, called bleed flows, is specified as mass flow outlet condition. All walls have been specified with no-slip boundary condition. One of the experimental test conditions, which is specified in Table-2, has been chosen for defining the boundary condition for the analysis. All the modified configurations are also given the same inlet boundary condition, so that one-to-one comparison of result is possible.

Solution Methodology

The 3-D, steady Navier-Stokes, energy and turbulence equations are cast into finite volume form and solved using pressure based method. This formulation permits the use of computational cells with arbitrary polyhedral cell topology including quadrilateral, hexahedral, triangular, tetrahedral, pyramidal, prismatic and hybrid meshes. This is useful as the geometry in hand is extremely complex.

Table-2 : Experimental Condition Used for Analysis

	Unit	
Inlet Total Pressure	kPa	1283
Inlet Total Temperature	K	712
Bleed 1	% of Combustor Inlet Mass Flow	7.6
Bleed 2		4.6
Bleed 3		5.2
Customer Bleed		0.3

Turbulence Model

In one of the earlier studies [9], standard k-ε model was used for modeling turbulence. Even though the result of pressure loss prediction was consistent with the experimental results, the loss was over-predicted by almost 2%. In the present study, turbulence is modeled using Realizable k-ε model, as this method takes into account the positivity of the normal stresses and is appropriate in the jet and recirculation regime. Validation of the model with experimental result has been carried out and there was a very good match between the experimental results and the model prediction [10]. The default model constants available in FLUENT have been used [15]. Turbulence intensity of 5% and hydraulic diameter at the combustor inlet has been specified. As the variation of y+ value is very wide, in the combustion chamber, enhanced wall treatment has been used.

Results and Discussion

Isothermal analyses have been carried out for the baseline model as well for the four modified configurations. The velocity contour plots, mass flow through the primary, secondary and dilution holes and the overall combustor total pressure loss for comparison.

Figure 8 shows the velocity vector plot in the primary zone of the combustor. The scale is not shown as the velocity data is classified. It shows that the primary zone recirculation pattern is not strong, as the jet angle is more than 90-degrees. The chute in the primary hole will guide the jet for certain depth, enhancing the jet velocity and making the jet perpendicular to the core flow.

The velocity contours at the mid section of the combustor, i.e. the plane passing through the atomizer, for the baseline model and for model-1 to model-4 are given in Fig.9a through Fig.9e. The velocity is represented in non-dimensional form, as ratio of local velocity to the inlet velocity. In this mid-section plane, passing through the atomizer, only primary and dilution holes are visible and as the secondary holes are staggered and not in-line with the atomizer, refer Fig.2, it is not seen. As the size of the secondary hole is very small (~ 16% of primary hole area), the effect of it is not shown in the results.

It can be observed from Fig.9a and Fig.9b that the primary jet, both at inner as well as in the outer wall, has become straight, as chute has been introduced in the primary holes. The jet angle with horizontal for outer and inner primary jets has increased from 55° and 70° to 85° and 80° respectively. It can be observed that the depth of penetration also has increased in the case of model-1 compared to baseline model.

On introducing chutes in the dilution zone in addition to the primary zone, (model-2), the velocity contour is shown in Fig.9c and it can be compared with the baseline model (Fig.9a) and model-1 (Fig.9b). The angle of the dilution jet and the depth of penetration have marginally increased compared to model-1 and the difference is not appreciable.

The velocity contour of model-3 (no chutes, but the dilution holes moved upstream to the plane of secondary holes) is similar to the baseline model as far as the depth of penetration of the jets and the angle of jets are concerned. But it can be seen, from Fig.9d that the outer primary jet angle is such that it affects the outer dilution jet.

Velocity contour plot of model-4 is shown in Fig.9e. It can be seen that the jet angle and the depth of penetration are similar to model-2.

Figure 10 shows the velocity vector plot in the primary zone of model-4. It can be seen that the primary zone recirculation pattern is not strong, and it has changed due to introduction of chutes. The jet angle has improved and it is almost 90 degrees to the core flow. The two opposing jets of primary zone, outer and inner primary jets are directed towards each other and it meets at approximately at the mid-point of the flame tube. The vector plot shown in Fig.10 is an improved one compared to baseline configuration shown in Fig.8.

The massflow split across the annuli and the core has been estimated and compared for all the configurations and they are tabulated in Table-3. The flow split is specified as the percentage of the combustor inlet flow. The flow split almost remained same in model-1 and model-2, as compared to model-0, mainly because the flow area of the liner holes is the same, even though the chutes are introduced. However, the outer annulus flow has reduced and the inner annulus flow has increased with minor reduction in the core flow, in the case of model-3 and model-4. This can be attributed to elimination of secondary holes in the liner and shifting the dilution to the plane of secondary holes.

The overall total pressure loss across the combustor is computed by taking the total pressure at the combustor inlet and exit plane. The overall combustor total pressure loss comprises of diffuser loss and liner loss. The diffuser loss goes as a loss to the system, where as the liner loss is useful for combustion process. If the primary or dilution jet velocities are increased, it is accompanied by corresponding increase in liner pressure loss. However, this increased jet velocity results in increasing the flame tube turbulence levels, which is beneficial for better mixing and combustion. The annulus loss and overall combustor loss is derived from the results of simulation and the liner loss is computed as the difference of combustor loss and diffuser loss. The pressure losses for various configurations are given in Table-4.

As chutes are introduced in model-1 and model-2, the effective area available in the primary and dilution holes will be reduced leading to more flow resistance and increased liner loss, as well as combustor loss, which is seen from Table-4.

Table-3 : Mass Flow Split Across the Annuli and the Core

	Outer Annuius	Inner Annuius	Core
	Deviation of Flow Split from Baseline Data, as % of Inlet Flow		
Model-0	Baseline		
Model-1	+0.4	-0.3	-0.1
Model-2	-0.1	-0.4	+0.5
Model-3	-2.8	+3.3	-0.5
Model-4	-2.8	+3.3	-0.5

Table-4 : Deviation of Percentage Total Pressure Loss Across Various Models

	Outer Annulus in %	Inner Annulus in %	Average Diffuser Pressure Loss in %	Overall Combustor Pressure Loss, in %	Liner Pressure Loss, in %
Model-0	Baseline				
Model-1	+0.08	+0.07	+0.07	+0.52	+0.45
Model-2	+0.43	+0.31	+0.37	+0.96	+0.59
Model-3	+0.06	-0.16	-0.05	-0.25	-0.19
Model-4	+0.05	-0.16	-0.055	+0.32	+0.38

Comparison of overall total pressure loss across the combustor for all the models reveal that the model-3 has the least pressure loss which is lower than the baseline model. Even though model-4 gives marginally higher pressure loss as compared to baseline model, the values are less than model-1 and model-2. It can be seen that the pressure loss up to the annuli also has reduced marginally in the case of model-3 and model-4. Particularly, the annulus pressure loss reduction in the inner annulus is more than the outer annulus and this may be the reason for the increased inner annulus mass flow, as observed in Table-3.

In the case of model-3 and model-4, the secondary hole has been closed leading to reduction of open hole area in the liner. This will increase the jet velocity and liner pressure loss as well. The isothermal flow result shows that model-4 has advantage over the baseline, as the velocity contour plot shows that the primary jet penetration is, as desired. As model-4 has better jet penetration, and comes with a penalty of marginally increased pressure loss, it is considered as meeting the design requirements. However, analysis with chemical reaction only can reveal the effect of these changes on the temperature distribution. Further study with chemical reaction is being carried out.

Conclusion

The flow field in a practical aero gas turbine combustor under isothermal condition has been studied. Complete combustor geometry, starting from compressor exit to turbine inlet, has been modelled using hexahedral dominant grid. All the complicated features of the combustor, including the swirler, have been modelled. Based on the isothermal flow analysis results of the baseline configuration, changes had been made to various air injection holes of the combustor liner, to improve the flow field. The primary and dilution holes are modified by providing chutes, to improve the jet penetration and the angle of jet. Four different configurations has been studied and compared with the baseline configuration. Overall total pressure loss across the combustor has been calculated and compared for various configurations. The modification marginally affected the mass flow distribution across the outer and inner annuli and also a small change in overall combustor pressure loss is observed. It is found that model-4, among other configurations, shows better results in spite of indicating slightly elevated pressure loss than the baseline configuration.

Acknowledgement

The authors would like to thank the Director, GTRE for his constant support and encouragement in pursuing the work. The authors would also like to thank the officers and staff of Combustion Group and CFD Group of GTRE for participating in useful technical discussions.

References

1. Anand, M.S. and Priddin, C.H., "Combustion CFD - A Key Driver to Reducing Development Cost and Time", Fifteenth International Symposium on Air Breathing Engines, Bangalore, India, ISABE 2001-1087.

2. Crocker, D.D., Nickolaus, D. and Smith, C.E., "CFD Modeling of a Gas Turbine Combustor from Compressor exit to Turbine Inlet", ASME-98-GT-184, Journal of Engineering for Gas Turbines and Power, Vol.121, January 1999, pp 89-95.

3. Liu, N. S., Shih, T. H. and Wey, T., "Comprehensive Combustion Modeling and Simulation: Recent Progress at NASA Glenn Research Center", ISABE-2007-1268.

4. Motsamai, O.S., Visse,r J.A., Morris, M. and De Kock, D.J., "An Efficient Strategy for the Design Optimization of Combustor Exit Temperature Profile", GT2006-91325, ASME Turbo Expo 2006, Power for Land Sea and Air, May 8-11, 2006, Barcelona, Spain.

5. Tangarila, V., Tolpadi, A., Danis, A. and Mongia, H., "Parametric Modeling Approach to Gas Turbine Combustor Design", ASME IGTI Conference 2000, 2000-GT-0129.

6. Carrotte, J.F., Griffithe, J.P. and Spencer, A., "Primary Jet Characteristics within an Isothermal Gas Turbine Combustor", ASME Paper 2001, 2001-GT-0057.

7. McGuirk, J.J. and Spencer, A., "Coupled and Uncoupled CFD Prediction of the Characteristics of Jets from Combustor Air Admission Ports", ASME Paper 2000, 2000-GT-125.

8. Sivaramakrishna, G., Muthuveerappan, N., Venkataraman Shankar and Sampathkumaran, T.K., "Combustor Geometry Optimization Studies Using CFD Techniques", Fifteenth International Symposium on Air Breathing Engines, Bangalore, India, ISABE-2001-1089.

9. Sivaramakrishna, G., Muthuveerappan, N., Venkataraman Shankar, Sampathkumaran, T.K., "CFD Modeling of the Aero Gas Turbine Combustor", Proceedings of ASME Turbo Expo 2001, 2001-GT-0063.

10. Srinivasa Rao, M., Sivaramakrishna, G., Muthuveerappan, N., Kishore Kumar, S. and Venkataraman Shankar., "CFD Analysis of an Aero Gas Turbine Combustor -Validation and Experiments", Proceedings of ICONICE-2007, Hyderabad, India, pp. 813-817.

11. Eccles, N.C. and Priddin, C.H., "Accelerated Combustion Design Using CFD", 1999, XIV ISABE Paper 99-7094.

12. Birkby, P., Cant, R.S., Dawes, W.N., Demargne, A.A.J., Dhanasekaran, P.C., Kellar, W.P., Rycroff, N.C., Savill, A.M., Eggels, R.L.G.M. and Jennions, I.K., "CFD Analysis of a Complete Industrial Lean Premixed Gas Turbine Combustor", ASME Paper 2000-GT-131.

13. Lai, M.K., Reynolds, R.S. and Armstrong, J., "CFD-Based, Parametric, Design Tool for Gas Turbine Combustors from Compressor Deswirl Exit to Turbine Inlet", 2002, ASME Paper GT-2002-30090.

14. Lefebvre, A.H., "Gas Turbine Combustion", Hemisphere Publishing Corp, USA, 1993.

15. "FLUENT 6.2 User Guide", 2006, Lebanon, NH, USA, Fluent Inc.

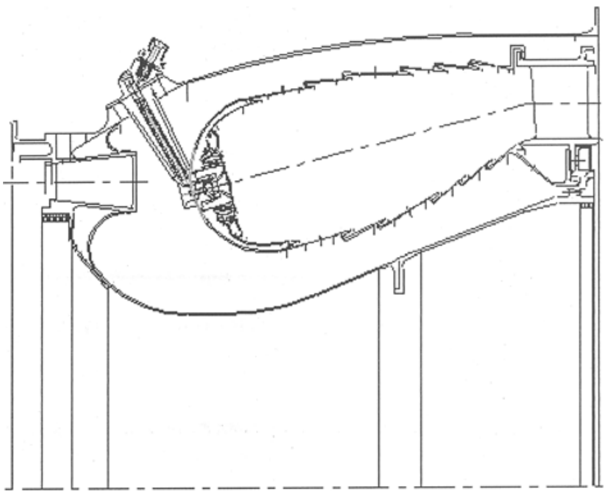

Fig.1 Cross-Section of Combustor - Original Configuration

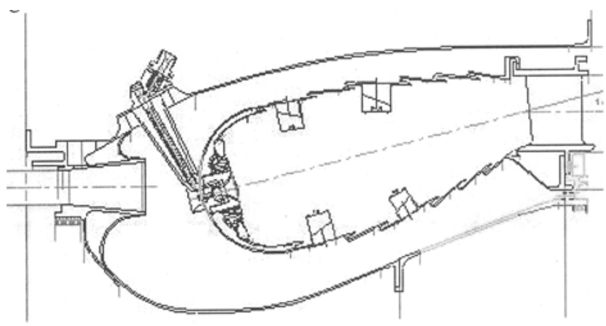

Fig.3 Cross-Section of Combustor Showing the Chutes

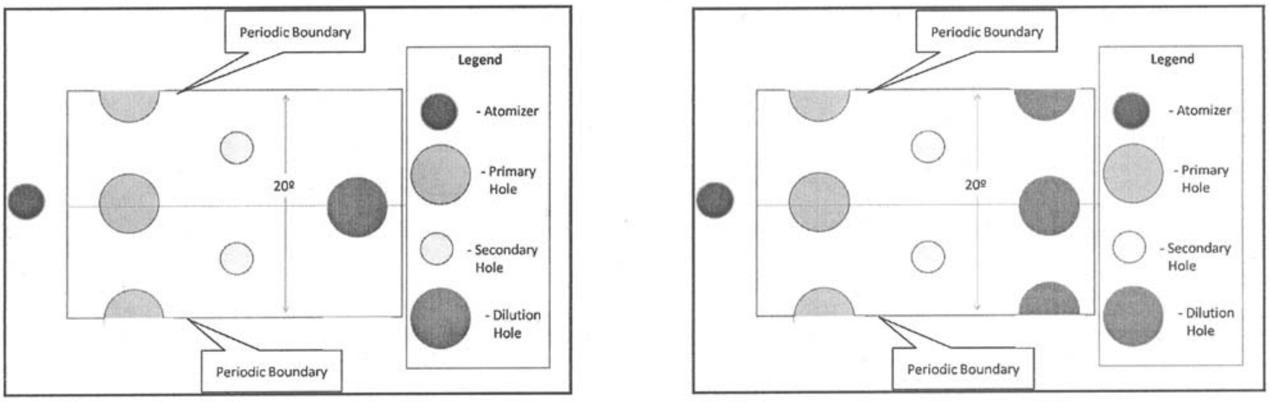

Outer Liner **Inner Liner**

Fig.2 Disposition of the Primary, Secondary and Dilution Holes on Outer/Inner Linear

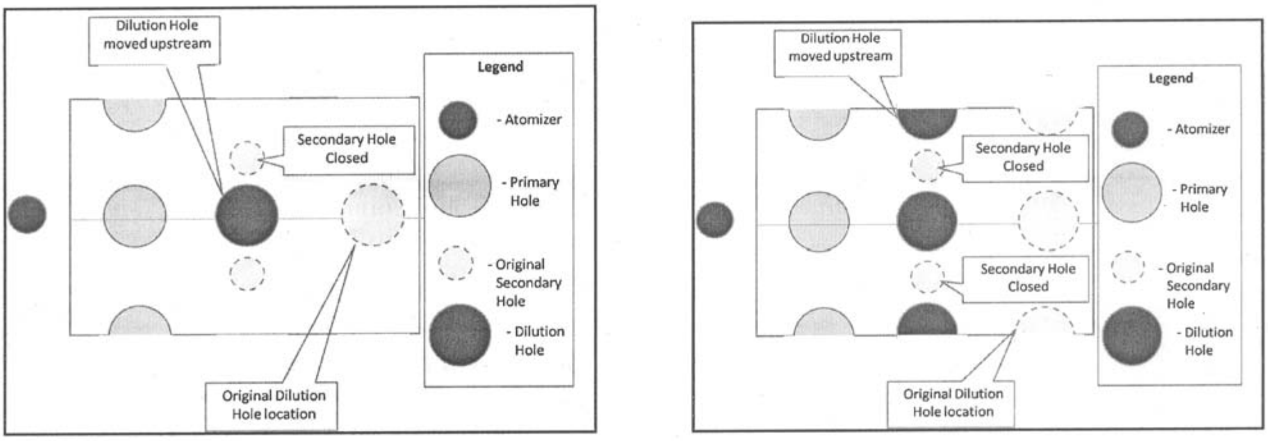

Outer Liner **Inner Liner**

Fig.5 Disposition of the Primary and Dilution Holes on Outer/Inner on Model-3 or Model-4

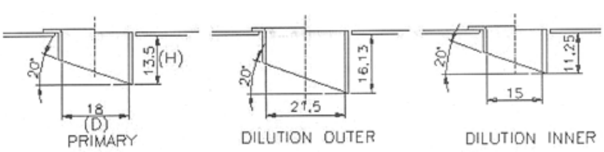

Fig.4 Geometric Details of Chutes

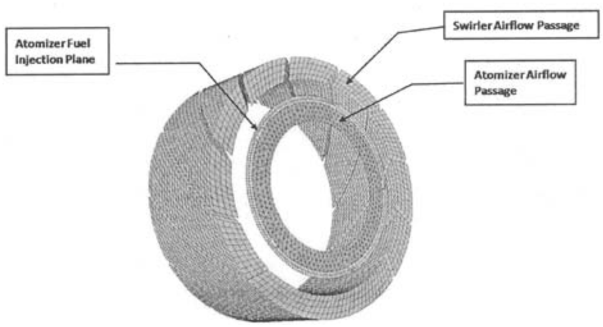

Fig.7 Mesh Passing Through the Swirler

Fig. 6 Mesh used for the Combustor Analysis

Fig.8 Velocity Vector Plot of Model-0 at the Plane Passing through Atomizer

Fig.9a Velocity Contour Plot of Model-0

Fig.9b Velocity Contour Plot of Model-1

Fig.9c Velocity Contour Plot of Model-2

Fig.9d Velocity Contour Plot of Model-3

Fig.9e Velocity Contour Plot of Model-4

Fig.10 Velocity Vector Plot of Model-4 at the Plane Passing Through Atomizer